Biomass Conversion and Biorefinery (2022) 12:913–923
https://doi.org/10.1007/s13399-020-01222-x

ORIGINAL ARTICLE

Sustainability and application of corncob-derived biochar for removal of fluoroquinolones

Bao-Trong Dang[1] · Obey Gotore[1] · Rameshprabu Ramaraj[2] · Yuwalee Unpaprom[3] · Niwooti Whangchai[4] · Xuan-Thanh Bui[5,6] · Hideaki Maseda[7] · Tomoaki Itayama[1]

Received: 27 October 2020 / Revised: 3 December 2020 / Accepted: 14 December 2020 / Published online: 23 February 2021

Abstract

Biochar-inspired tertiary removal system is beneficial in preventing antibiotic residue discharged from hospital wastewater treatment. Taking advantage of a simple kiln controlled at around 600 °C, we succeeded in carbonizing corncobs to biochar with a surface area of 306 m^2/g. Using ciprofloxacin (CFX), ofloxacin (OFX), and delafloxacin (DLX), we demonstrated the performance of the corncob biochar for the sorption removal. The pseudo-second-order rate of DLX was lower than CFX and OFX. The maximum sorption capacity Q_{max} of 93.9 μg/g for DLX, 399.6 μg/g for CFX, and 306.0 μg/g for OFX were estimated using the Langmuir model. The parameter K_L relating to binding strength for DLX is 8 times larger than CFX and OFX. The Q_{max} could be mainly determined by the pore size distribution of the biochar and the dimensions of FQs considering hydration. Furthermore, we discussed that these results might relate to the number of halogen atoms and functional groups in the fluoroquinolones.

Keywords Biochar · Delafloxacin · Fluoroquinolones · Sorption · Isotherm · Kinetics

1 Introduction

Fluoroquinolones (FQs) are a powerful synthesis class antibiotic currently receiving attention due to low biodegradability, which significantly impacts the ecosystem. For instance, the residues FQs such as ciprofloxacin (CFX) has been routinely detected from hospital effluents such as 0.6–53.3 μg/L (Vietnam) [1], 32–99 μg/L (Brazil) [2], and up to 2.2–236.6 μg/L (India) [3]. Conventional biological wastewater treatment did not design to completely remove FQs [4]. Different technologies have been launched to examine potential removal, such as the adsorption process using magnetite/silica/pectin nanoparticles [5], wetland [6], and MBR [7]. In addition, Sponge-MBR was tested for hospital wastewater treatment [8]. However, the incomplete removal resulting in a significant amount of antibiotics (6.5–13 μg/L) in the treated water still being discharged, adding a post-treatment system, is imperative for enhancing antibiotic removals. The spread of antibiotic pollution resulting from incomplete wastewater treatment can be accompanied by disruption of microbial communities and the generation of antibiotic resistance–carrying bacteria (ARBs), which is of most significant concern as a current environmental pollution problem [9].

✉ Tomoaki Itayama
itayama@nagasaki-u.ac.jp

1 Graduate School of Engineering, Nagasaki University, 1-14 Bunkyo-machi, Nagasaki 852-8521, Japan

2 School of Renewable Energy, Maejo University, Chiang Mai 50290, Thailand

3 Program in Biotechnology, Faculty of Science, Maejo University, Chiang Mai 50290, Thailand

4 Faculty of Fisheries Technology and Aquatic Resources, Maejo University, Chiang Mai 50290, Thailand

5 Key Laboratory of Advanced Waste Treatment Technology, Vietnam National University Ho Chi Minh (VNU-HCM), Linh Trung ward, Thu Duc district, Ho Chi Minh City 700000, Vietnam

6 Faculty of Environment and Natural Resources, Ho Chi Minh City University of Technology (HCMUT), Ho Chi Minh City 700000, Vietnam

7 Biomedical Research Institute, National Institute of Advanced Industrial Science and Technology, 1-8-31 Midorigaoka, Ikeda, Osaka 563-8577, Japan

In general, building post-treatment systems with cost-effective and easy to manufacture and maintain locally is essential. An adsorption method using biochars derived from agricultural wastes increases attention [10–13]. Corn is one of the most important crops produced worldwide, grown in 165 countries, and has yielded approximately 1016 million tons [14]. The leaves, stem, and corncob from agricultural activities are valuable materials for locally available industrial applications. When a slow pyrolysis process was applied at temperatures above 500 °C, the corncobs were transformed into stable biochar [15]. Corncob biochar was emphasized as a potential sorbent for pesticide and herbicide removal [16, 17]. However, the application of corncob biochar for FQ removal has not been thoroughly investigated yet [18]. In contrast, diversity biomass–derived biochar has been tested for potential FQ removal [10], tetracycline [12], and sulfonamide [11].

Usually, the biochar is carbonized using an electric furnace with high-precision temperature control in the laboratory. It is crucial to produce biochar in more realistic rural areas without electricity and complex reactor configuration. The particle size of produced biochar is certainly too small to establish post-filtration treatment, such as less than 0.85 mm [19] and 0.15 mm [20]. Another critical point of view is to set an appropriate antibiotic concentration for each adsorption experiments [21]. Since laboratory adsorption experiments to characterize biochar were often performed at higher concentrations than the environment, we cannot evaluate practical application's true removal capability [22].

In this study, we aimed to elucidate the adsorption properties of ciprofloxacin, ofloxacin by corncob biochar produced by simple kilns manufactured in developing countries. Our adsorption experiments were then conducted at concentrations that reflected the actual application conditions for removing FQs in hospital wastewater. We also examined the adsorption of a novel delafloxacin as the newest FQ compared to ciprofloxacin and ofloxacin as conventional FQs, because DLX showed extreme toxicity in vitro than other FQs [23]. Moreover, we anticipate increasing delafloxacin prescriptions in developing countries concerning its potent therapeutic [24].

2 Materials and methods

2.1 Production and characterization of biochar

The pyrolysis of corncobs was performed using a simple kiln (Fig. 1) in the Bio-Energy research center at Maejo University, Chiang Mai, Thailand. The corncobs obtained from a farmer were naturally dried outdoor for 1 week to remove excess moisture (Fig. 2a). A steel can of about 20 L was used as a pyrolysis reactor to which dried corncobs of 1.7 kg were stuffed. The firewood of about 20 kg was burned in the kiln. The temperature was monitored by a thermocouple sensor (K-type, HTK0251, HAAKO Electric Co., Ltd., Japan). A digital temperature controller (E5CB, Omron Co., Japan) was used as a thermometer. Then, the kiln was heated for about 2 h, and the temperature was manually controlled at around 600 °C by controlling air supply (Fig. 3). After the pyrolysis, the weight of carbonized corncobs was measured. Next, the carbonized corncobs (Fig. 2b) were milled and passed two mesh size sieves to obtain particles of approximately 1.5–3 mm in diameter. The biochar was washed with tap water and deionized water. The wash water changed from pH 9.6 to pH 7.2 due to removing the remaining ash. The corncob biochar was dried in an oven at 105 °C for 2 h. We observed the dried corncob biochar using a scanning electron microscope (HITACHI TM3030Plus, Japan).

2.2 Experiments on iodine adsorption

The dried corncob biochar of around 5 g was agitated in a 500-mL beaker with ultra-pure water; then, it was set in a decompressed chamber for a half-day using a magnetic stirrer to expel air in pores. Water content wt (%) of the wet biochar was measured ($n = 5$) using the dry oven at 105 °C for 2 h to calculate the dry weight. Two Erlenmeyer flasks of 500 mL contained 50-mM and 25-mM iodine solutions of 250 mL. Each iodine solution was diluted from a 0.5-M iodine solution (Nacalai Tesque, INC, Japan). Then, biochar of 3.93 dry-g and 3.94 dry-g were put to the 50-mM flask and the 25-mM flask. Each flask was rotated with 140 rpm at 20 ± 1 °C for 48 h using a thermostatic shaker (BIO-Shaker BR-40LF, TAITEC, Co., Japan). Ten milliliters of sample water was collected from each flask at 0, 1, 2, 4, 12, 24, 36, 42, and 48 h after the start of shaking. The iodine concentration in each sample was measured by a titration method by sodium thiosulfate solution of 0.1003 M (Nacalai Tesque, INC, Japan). This titration was performed by the standard method of iodine adsorption on activated carbon [25]. Since the volume V_j decreased by each sample collection, we estimated the adsorbed quantity of iodine ADI_k (mol) as follows:

$$\mathrm{ADI}_k = \sum_{j=1}^{k} \left(C_{j-1} - C_j\right) V_{j-1}, k = 1, 2, 3, \ldots, 9 \quad (1)$$

where $V_0 = 0.25$ L, $V_2 = 0.24$ L, …, $V_8 = 0.17$ L, iodine concentration C_j (mmol) at each time 0 h (j = 1), 1 h (j = 2), …, 48 h (j = 9).

To obtain the adsorption isotherm, we prepared 8 Erlenmeyer flasks of 100 mL with iodine solutions of 20 mL of 0.005 mM, 0.01 mM, 0.02 mM, 0.04 mM, 0.08 mM, 0.125 mM, 0.16 mM, and 0.25 mM with the biochar of 0.24 g, 0.24 g, 0.23 g, 0.24 g, 0.24 g, 0.23 g, 0.23 g, and 0.23 g as dry weight, respectively. Then, three flasks were prepared to control no biochar to evaluate the iodine adsorption on the flask's surface. Each flask was rotated with 140 rpm at 20 ± 1 °C for 48 h.

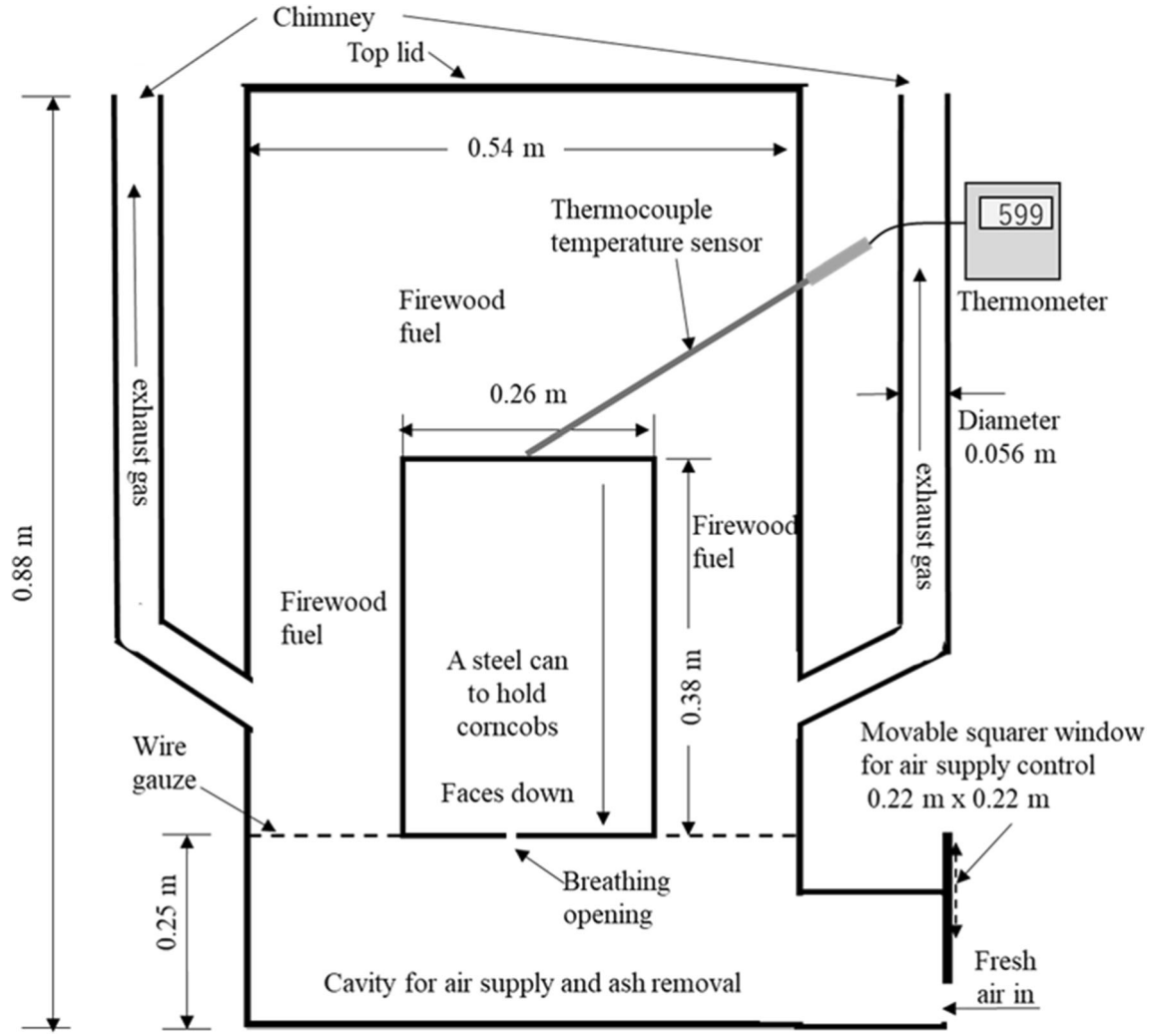

Fig. 1 Configuration of a kiln for pyrolysis of corncobs. The kiln has a cavity of 120 L for firewood and a steel can of 20 L. The movable square widows can be up and down to control the air supply for temperature control

2.3 Experiments on FQ adsorption

Ciprofloxacin (LKT Laboratories Inc., St. Paul, MN, USA), and ofloxacin (Wako Pure Chemical Industry, Ltd., Tokyo, Japan) and delafloxacin (Sigma Aldrich, St. Louis, MO, USA) were purchased. Each stock solution of each FQ of 50 mg/L was prepared by dilution using ultra-pure water (PURELAB flex 2, ELGA Lab Water, UK). CFX, OFX, and DLX of 500 mL (250 μg/L) in Erlenmeyer flasks of 1 L were prepared with 0.65 g (dry) biochar. Each flask was rotated with 140 rpm at 20 ± 1 °C for 48 h using a thermostatic shaker (BIO-Shaker BR-40LF, TAITEC Co, Japan). Thirty-seven milliliters of sample water was collected from each flask at 2, 5, 10, 20, 40, and 80 min, then 4, 8, 12, 24, and 48 h after the start of shaking. We used Eq. (1) for the kinetics data analysis as well as the iodine.

Adsorption isotherm experiments of three FQs were performed using eight different initial concentrations of 100, 200, 300, 400, 600, 800, 1000, and 1200 μg/L. Biochar of 0.054 g (dry) was placed in each 100 mL Erlenmeyer flask containing 50 mL of each different concentration FQ solution. All flasks were rotated with 140 rpm at 20 ± 1 °C using the same thermostatic shaker. Finally, 48 mL of each sample water was collected after shaking for 24 h for HPLC analysis.

HPLC analysis method was modified from a previous study. The detail is described in the supporting information.

2.4 Data analysis

In the kinetics experiments, we used the pseudo-first-order (PFO) model and pseudo-second-order (PSO) model [26] as follows:

$$\text{PFO}: q_t = q_{\max}\left(1-e^{-k_1 t}\right) \tag{2}$$

$$\text{PSO}: q_t = \frac{k_2\, q_e^2\, t}{1 + k_2 q_e\, t} \tag{3}$$

where q_t (μg/g) is the adsorption amounts, k_1 (h^{-1}) and k_2

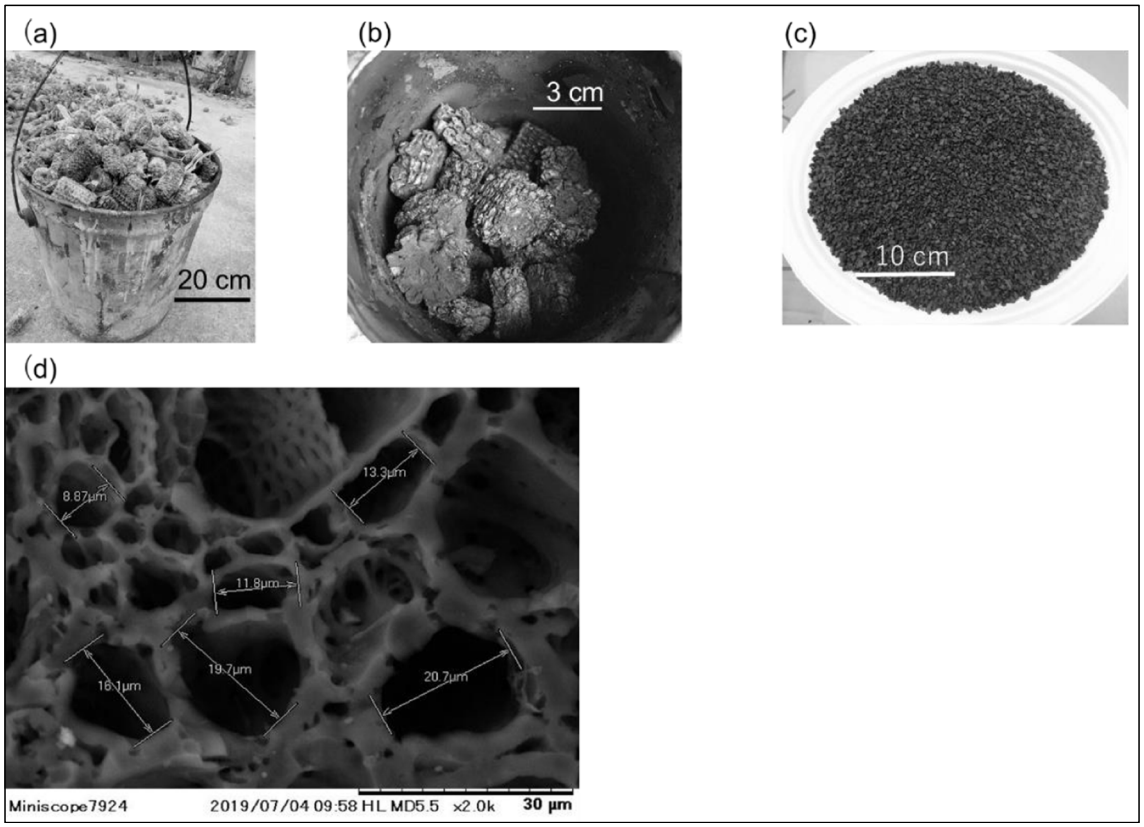

Fig. 2 The photos of **a** dry corncobs, **b** carbonized corncobs, **c** crashed granular biochar, and **d** SEM image of the corncob biochar (15 kV)

(g μg^{-1} h^{-1}) are the rate constants of PFO and PSO, and q_{max} (μg/g) and q_e (μg/g) are the maximum amounts of adsorption.

In the adsorption isotherm experiments, Langmuir model and Freundlich model were used.

$$\text{Langmuir}: q_e = \frac{Q_{max} K_L C_e}{1 + K_L C_e} \quad (4)$$

$$\text{Freundlich}: q_e = K_F C_e^n \quad (5)$$

where q_e (μg/g) is the adsorption capacity per unit mass adsorbent at the equilibrium, Q_{max} (μg/g) is the maximum adsorption capacity, and K_L (L/μg) is the surface adsorption affinity constant. C_e (μg/L) is the adsorbate concentration in aqueous solution at the equilibrium, K_F (μg^{1-n} L^n/g) is the Freundlich coefficient, and n is the dimensionless number as the Freundlich empirical constant.

We compared the goodness of two non-linear models in the adsorption kinetics and the adsorption isotherm based on Akaike information criteria (AIC) [27]. All non-linear regressions were performed using nls() function in statistical computing software R (ver.3.6.1) (http://www.rstudio.com/.)

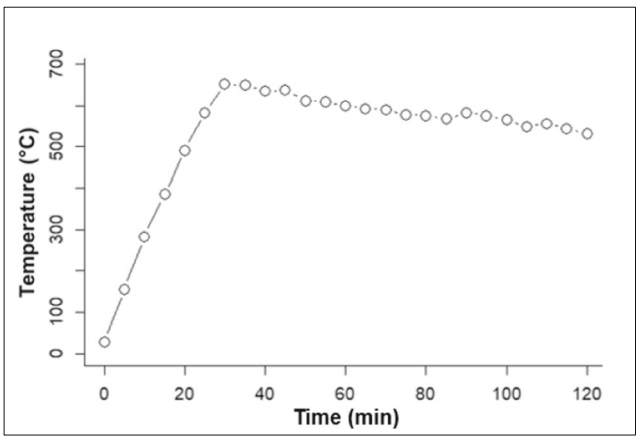

Fig. 3 Change of temperature in the kiln during the pyrolysis process

3 Results and discussion

3.1 Production and characterization of corncob biochar

The temperature inside the kiln rose for 30 min and then reached about 650 °C; then, it gradually decreased to 520 °C at 2 h after the start, as shown in Fig. 3. The control of pyrolysis temperature significantly produces good quality biochar [16]. Higher temperature settings than optimal temperature can reduce functional groups such as -COOH and -OH and increase the aromatic C fraction in corncob biochar [15]. The high microporous corncob biochar could be achieved in the range of 500–600 °C [15]. This study successfully retained

temperature in the kiln from 650 to 530 °C for 90 min. On the other hand, the biochar yield was approximately 25% of the total of 1.7-kg corncobs. This yield is comparable in the previous study [28].

Around 20 kg of firewood was totally consumed to obtain the biochar of 420 g. The carbonized corncobs were milled and sieved to achieve particles of corncob biochar from 1.5 to 3 mm in diameter, as shown in Fig. 2c. In this study, we used a bigger particle comparing to other research, as mention beforehand. In general, powder biochar is useful as an adsorbent. However, biochar particles that are too small are not suitable to make a column reactor because sufficient water permeability is required. Also, it is actually reported that biochar particles of 1–5 mm in size could effectively remove pharmaceutically active compounds [29]. The SEM image on the corncob biochar in Fig. 2d presented the porous structure. Each pore's diameter is typically less than about 30 μm that is the same pore size as a previous study [17].

3.2 The iodine adsorption experiments

We performed iodine adsorption experiments to evaluate the surface area of the produced corncob biochar as an adsorbent. First of all, we needed to determine the adequate time to achieve the adsorption equilibrium. Changes of iodine adsorption on the corncob biochar were shown in Fig. 4a. It was found that the control flask without biochar also adsorbed a small amount of iodine in 42 h and 48 h. Thus, the plots on the amounts of adsorbed iodine for 50 mM and 25 mM initial iodine concentrations were subtracted from the control's adsorbed iodine. Non-linear regression using PFO model resulted in the estimation value of the rate constant $k = 0.136 \pm 0.050$ h^{-1} in Eq. (2) for the 50 mM iodine and $k = 0.128 \pm 0.042$ h^{-1} for the 25 mM. The characteristic time (= $1/k$) was calculated as 7.33 h (50 mM) and 7.78 h (25 mM), respectively. The adsorption isotherm experiment was incubated for 48 h, as six times the characteristic time is a reasonable time to reach equilibrium. The solid curve on the plot shows the Langmuir model fitted by non-linear regression, as shown in Fig. 4b. The parameters $Q_{max} = 2.424 \pm 0.188$ mmol/g and $K_L = 83.004 \pm 30.494$ L/mol in Eq.(4) were estimated.

Langmuir model principally assumes single-layer adsorption on the adsorbent. Therefore, the corncob biochar's surface area can be calculated from the maximum number of iodine molecules adsorbed on the biochar. The maximum adsorbed iodine molecule is $1.46 \pm 0.11 \times 10^{21}$ (iodine atom per gram) was obtained. Mianowski et al. [30] estimated that iodine's surface area was 0.2096×10^{-18} (m^2 per iodine atom) from comparing the specific surface area by BET method and the iodine adsorption number on activated carbon. Thus, the surface area of 306 ± 24 m^2/g is successfully estimated for corncob biochar using this iodine surface area. As reported, Liu et al. [15] estimated the 192 m^2/g by BET method for the corncob biochar obtained by the pyrolysis temperature of 600 °C and residence time around 1 h [15]. Rodriguez et al. [31] and Hao et al. [16] also reported 80.14 m^2/g (600 °C) and 25.6 m^2/g (650 °C and 1 h) based on the BET method, respectively. Generally, the difference in pyrolysis temperature, heating rates, residence time, and natural feedstock could shift biochar surface characteristics. Considering that a simple kiln was used for production in Fig. 1, the surface area of 306 m^2/g obtained is sufficient without any chemical modification, compared to the surface area of typical activated carbon of 1000 m^2/g. The biochar should rely on a straightforward way in production and enough quality to approach developing countries; an intricate process or chemical treatment and its by-product could ground a decline in meaningful of eco-friendly technology.

3.3 Sorption of the three fluoroquinolones

3.3.1 Results of sorption kinetics and equilibrium

Figure 5 presents astonishing results: adsorption of about 68% CFX and 70% OFX was achieved only 2 min after starting the kinetics experiment, respectively. DLX's adsorption was slower than CFX and OFX, but it was high enough as the adsorption rate reached 51% after 5 min. PFO and PSO models for kinetics analysis are represented by Eqs. (2) and (3). As shown in Table 1, the PSO model is a better model than the PFO model by AIC and RSE [32]. Each adsorbed amount q_e of CFX and DLX on the biochar at equilibrium state is estimated to 152.3 ± 1.8 μg/g and 106.4 ± 5.8 μg/g, respectively. Then, 1.01 ± 0.265 g μg^{-1} h^{-1} and 0.076 ± 0.030 g μg^{-1} h^{-1} are obtained as the constant rate sorption of CFX and DLX, respectively.

In the PSO model, each half-saturation time $t_{0.5}$ ($= k_2 q_e$) of 0.39 min, 0.15 min, and 7.42 min can be estimated for CFX, OFX, and DLX, respectively. Since the time constant $T_{99.5}$ to achieve 99.5% sorption for the equilibrium is estimated as 200 times of $t_{0.5}$, considering the Eq. (3), PSO and 200/201 = 0.995, 1.3 h, and 0.5 h are obtained for $T_{99.5}$ of CFX and OFX, respectively. These results were remarkably shorter than 4 or 6 h for CFX's sorption equilibrium time or other FQs [33]. On the other hand, there is no report to show DLX's sorption in previous studies to date. We succeeded firstly to elucidate the sorption character of DLX. The sorption equilibrium time $T_{99.5}$ of 24.7 h was revealed more than around twenty times longer than that of CFX or OFX.

They considered that this sorption equilibrium time of DLX, the incubation time of 24 h was adequate for the adsorption isotherm experiments. The results of the sorption isotherm experiments are presented in Fig. 6. AIC values in each FQs shown in Table 2 support that the Langmuir model is better. The maximum sorption capacities Q_{max} for CFX, OFX, and DLX are estimated to be 399.6 μg/g (1.21 μ mol/

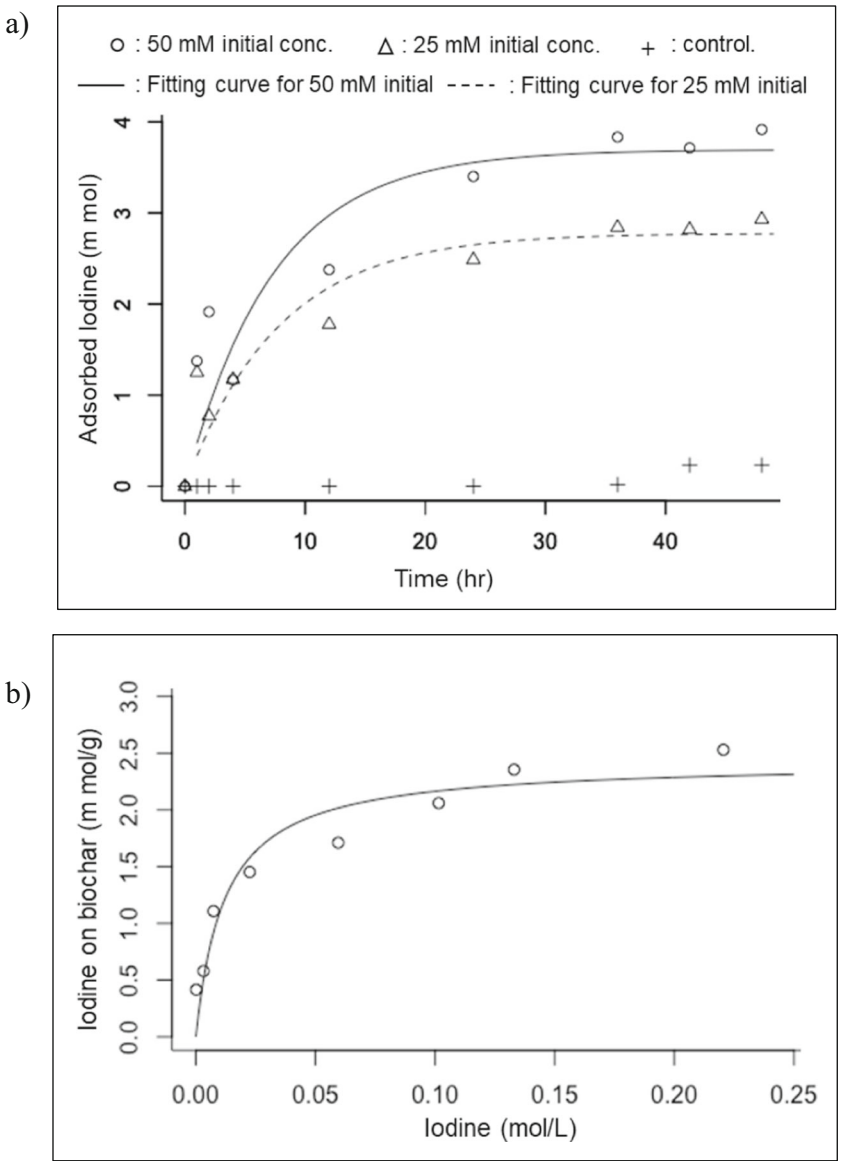

Fig. 4 **a** Time course of adsorption of iodine on the corncob biochar. **b** Adsorption isotherm of iodine on the biochar fitted by Langmuir model

g), 306.0 μg/g (0.85 μ mol/g), and 93.9 μg/g (0.21 μ mol/g), respectively. These results reveal that DLX's Q_{max} is about one-third to one-fourth of the Q_{max} of CFX and OFX.

Next, K_L of both CFX and OFX in Table 2 presents the same value 0.003 L/μg, and that for DLX is 0.024 L/μg, which is 8 times higher than CFX and OFX. The parameter K_L relates to the strength of binding (binding energy) between adsorbent and adsorbate [34]. Therefore, DLX's binding energy's experimental results are very high, but the maximum adsorption capacity is smaller than CFX and OFX are very interesting.

3.3.2 Discussion on sorption mechanism on corncob biochar

In this study, the obtained sorption capacities are smaller than the values in previous research. It was reported that CFX of 5 mg was adsorbed on 2-g biochar derived from rice husk [18]. One of the critical reasons for such a difference may be due to the different sizes of biochar. They used biochar with a small particle size of less than 0.4 mm compared to biochar from 1.5 to 3 mm in this study. However, large-sized particles are expected to enhance the filtration process's performance, considering clogging in practical application.

Regarding the sorption properties of FQs, the different antibiotic derivatives seem to influence the binding strength by altering mechanism interaction, including physical binding, π–π electron donor-acceptor (EDA) interactions, hydrogen bonding, ion exchange, and electrostatic interactions, and complexation [10, 35, 36]. In particular, DLX has more halogen atoms than CFX and OFX, which can significantly impact adsorption. Namely, the halogen atom with intense electron negativity can act as the strong electron acceptor in a

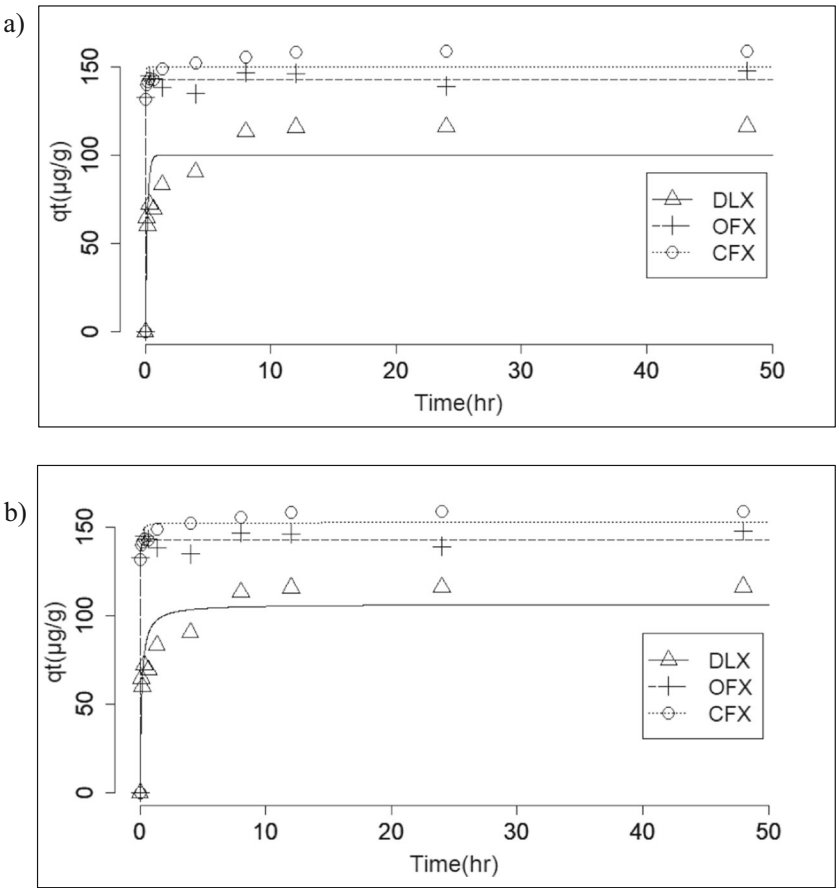

Fig. 5 Time course of adsorption of FQs on the corncob biochar and non-linear regression for the time course data using **a** pseudo-first-order model and **b** pseudo-second-order model

heteroaromatic ring [37]. Since the halogen atom can pull the π electron, π–π EDA interaction can be enhanced [38]. Both CFX and OFX have only one fluorine atom (Fig. 6a, b), while DLX has three fluorine and one chlorine, as shown in (Fig. 6c). Therefore, it is speculated that π–π EDA interaction between DLX and arene rings on the biochar surface can be

Table 1 Estimated parameters of PFO and PSO kinetics models for FQs on the corncob biochar

Models	Antibiotics	Parameters	Estimate	St. error	*p* value	AIC*
Pseudo-first-order $q_t = q_{max}\left(1-e^{-k_1 t}\right)$	CFX	q_{max} (μg/g)	149.9	2.2	1.6×10^{-14}	84.9
		k_1 (h^{-1})	60.782	11.246	2.9×10^{-4}	
	OFX	q_{max} (μg/g)	142.4	1.5	2.2×10^{-13}	61.7
		k_1 (h^{-1})	79.866	13.957	4.4×10^{-4}	
	DLX	q_{max} (μg/g)	100.1	6.9	1.5×10^{-7}	98.8
		k_1 (h^{-1})	6.212	2.153	2.2×10^{-2}	
Pseudo-second-order $q_t = \frac{k_2 q_e^2 t}{1+k_2 q_e t}$	CFX	q_e (μg/g)	152.3	1.8	2.1×10^{-15}	78.0
		k_2 (g μg^{-1} h^{-1})	1.01	0.265	3.3×10^{-3}	
	OFX	q_e (μg/g)	142.6	1.6	3.0×10^{-13}	61.9
		k_2 (g μg^{-1} h^{-1})	2.806	1.458	0.094	
	DLX	q_e (μg/g)	106.4	5.8	2.2×10^{-8}	92.3
		k_2 (g μg^{-1} h^{-1})	0.076	0.03	2.9×10^{-2}	

*The smaller the AIC, the better the model will be selected

Table 2 Estimated parameters of Langmuir and Freundlich models for FQs on the corncob biochar

Models	Antibiotics	Parameters	Estimate	St. error	*p* value	AIC*
Langmuir model $q_e = Q_{max} K_L \frac{C_e}{1+K_L} C_e$	CFX	Q_{max} (μg/g)	399.6	33	1.9×10^{-5}	68.9
		K_L (L/μg)	0.003	5.2×10^{-4}	1.7×10^{-3}	
	OFX	Q_{max} (μg/g)	306.0	15	1.2×10^{-6}	60.7
		K_L (L/μg)	0.003	4.6×10^{-4}	2.8×10^{-4}	
	DLX	Q_{max} (μg/g)	93.9	1.4	8.1×10^{-10}	40.1
		K_L (L/μg)	0.024	0.002	4.9×10^{-5}	
Freundlich model $q_e = K_F C_e^n$	CFX	K_F (μg^{1-n} L^n/g)	8.3	3.6	6.0×10^{-2}	77.1
		n	0.527	0.069	2.6×10^{-4}	
	OFX	K_F (μg^{1-n} L^n/g)	10.4	2.3	4.2×10^{-3}	64.8
		n	0.461	0.035	1.2×10^{-5}	
	DLX	K_F (μg^{1-n} L^n/g)	30.2	4.8	8.1×10^{-4}	53.5
		n	0.164	0.026	7.7×10^{-4}	

*The smaller the AIC, the better the model will be selected

stronger than between CFX (or OFX). The high electronegativity of fluorine and chlorine can also form hydrogen bonds with functional groups on the biochar [37, 39]. The total hydrogen bond acceptors such as O, N, Cl, and F attached to the DLX structure are higher than OFX and CFX (i.e., 11 > 8 > 7), respectively. This fact could contribute to establishing a hydrogen bond on biochar. Functional groups on biochar can also significantly affect the hydrogen bond formation and the cation exchange capacity [21, 40]. Carboxyl group contributes to hydrogen bonding interaction vis corncob biochar for 2,4-dichlorophenoxyacetic acid removal [17, 39]. The CFX structure and FQs contain a carboxylic group with pK_a of 5.90–6.23 and tertiary amine with pK_a of 8.28–8.89 [4]. At pH 7.2 of our experimental condition, the net charge of conventional FQs is negligible. However, DLX shows a negative charge because the secondary amine in the structure is removed, the primary amine in DLX's side chain does not show the protonation at neutral pH [41].

On the other hand, the Q_{max} of FQs is related to the effective surface area (ESA) of antibiotics. As with the iodine molecule, the actual ESA could be calculated from the occupied area of the adsorbed molecule and Q_{max}. Likewise, by using a CFX dimension of 1.35 × 0. 3 × 0.74 nm and OFX of 1.2 × 0.95 × 0.6 nm [42, 43], the occupied surface area for one CFX molecule is estimated of 1.00 nm^2 (= 1.35 nm × 0.74 nm), and for OFX molecule of 1.14 nm^2 (= 1.2 nm × 0.95 nm), respectively. The ESA for CFX (S_{CFX}) of 0.73m^2/g and OFX (S_{OFX}) of 0.58 m^2/g is estimated. Currently, no accurate molecular size data for DLX is available. However, the DLX dimensions of 1.21 nm^2 can be estimated under the assumption that the occupied area ratio for one molecule is proportional to the 2/3 power of the molecular weight ratio that MW_{CFX}:MW_{OFX}:MW_{DLX} = 331.34: 361.36: 440.7 (data PubChem) [4]. Therefore, the ESA for DLX (S_{DLX}) of 0.15 m^2/g is estimated. In addition, the order of molecular dimension (i.e., I_2 < CFX < OFX < DLX) correlates the inverse order of the occupying surface area (i.e., I_2 > CFX > OFX > DLX). The simple fact can qualitatively explain this relationship that smaller molecules can diffuse into smaller pores.

However, we have considered the ESA of iodine results is too high and distinct from three FQs (i.e., 306 > 0.73 > 0.58 > 0.15 m^2/g), respectively. For better understanding of this fact, we have to, of course, consider the pore size distribution of the biochar [16, 44, 45]. Although FQ's size is about 1 nm or more, FQ's hydration radius in water could influence the actual size of FQs. As already mentioned, more hydrogen bond acceptors in DLX than CFX and OFX can contribute significantly to the formation of thick hydrated layers. Therefore, it may be difficult for DLX to penetrate the micropore compared to CFX and OFX. Moreover, FQs contained much of the number of hydrogen bond acceptors (i.e., F, Cl, O, and N) as CFX of 7, OFX of 8, and DLX of 11 (data PubChem) could attribute to increasing FQ's hydration radius compared to iodine. Thus, high effective adsorption areas of iodine could be obtained. On the other hand, the slower the diffusion, the slower the adsorption rate, so it is considered that the hydration radius also affects the adsorption rate [34]. Then the diffusion coefficient D is inversely proportional to the molecule's dimension [46], given DEL is a slower sorption rate than OFX and CFX. However, to explain the kinetics rates of FQs quantitatively, it is necessary to determine radius of hydration of FQs. This knowledge is also vital for improving the adsorption properties of biochar for FQs, especially DLX. In future research, it is expected that the adsorption capacity will be significantly enhanced if the pyrolysis condition that can expand the pore diameter of charcoal to an appropriate size is possible concerning the hydration radius.

Finally, it should be mentioned that this experiment succeeded in producing biochar in a very simple kiln, which is easy for rural people in developing countries to build. Therefore, in order to lead to actual environmental improvement, it is important to show that biochars produced in such rural areas are effective as wastewater treatment materials in future research.

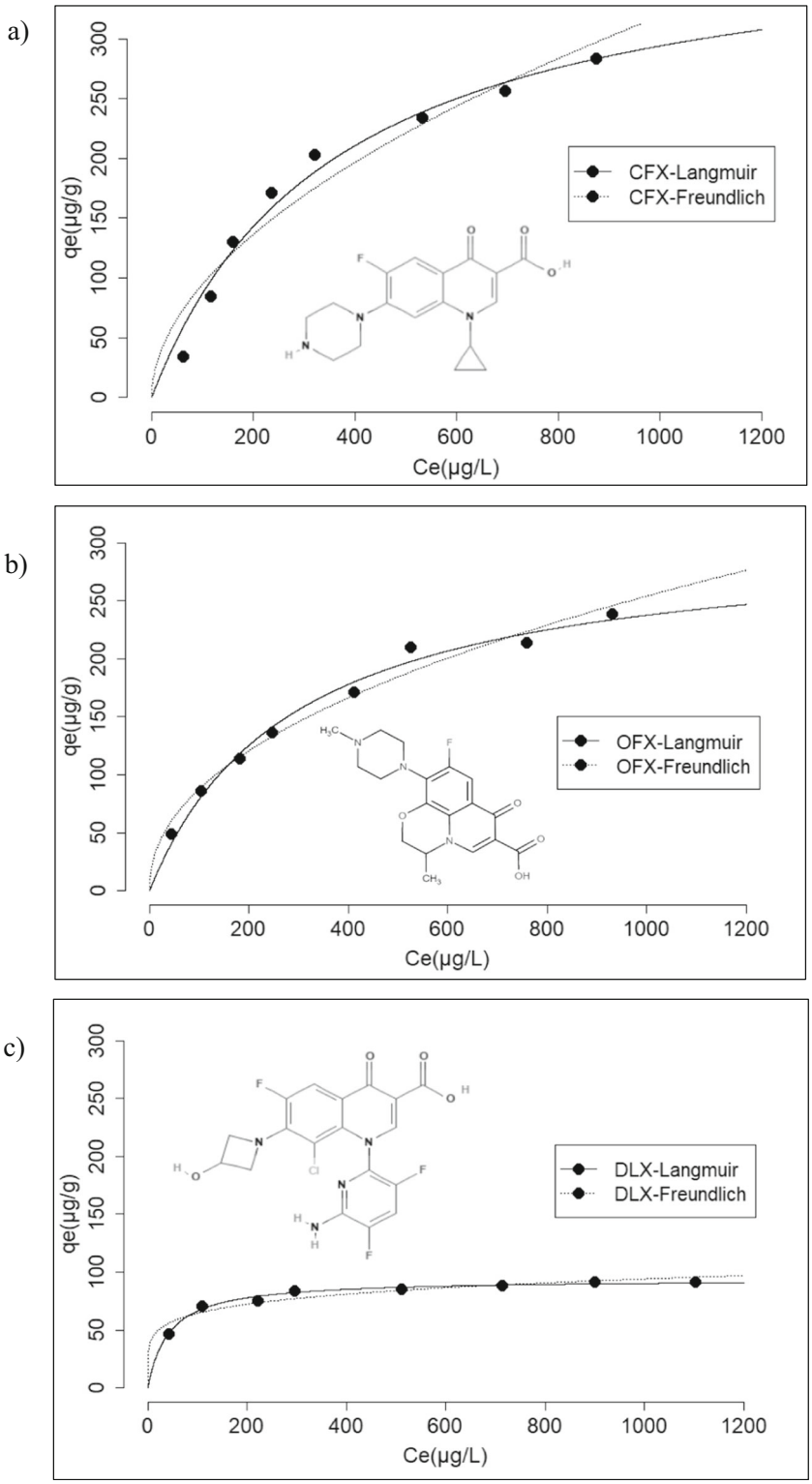

Fig. 6 Adsorption isotherm of FQs: **a** DLX, **b** OFX, **c** CFX, and non-linear regression using Langmuir and Freundlich models for the isotherm

4 Conclusions

We succeeded in obtaining corncob biochar with a large surface area of 306 m^2/g using a simple kiln and firewood for the carbonization. The pseudo-second-order model and Langmuir isotherm model were selected as a better model for the sorption kinetics and the sorption isotherm of the biochar for three fluoroquinolones CFX, OFX, and DLX. The kinetics sorption rate constant of DLX was significantly smaller than CFX and OFX. The maximum sorption capacity Q_{max} for DLX of

93.9 μg/g is lower than CFX (399.6 μg/g) and OFX (306.0 μg/g). On the other hand, the parameter K_L, which relates to binding strength in the Langmuir model, for DLX is 8 times larger than CFX and OFX. We speculated that the maximum sorption capacity could be mainly determined by the pore size distribution of the corncob biochar and the molecular dimensions of FQs considering hydration. Finally, we discussed that these results might relate to the higher number of halogen atoms in DLX than in CFX and OFX; then, the difference of function groups and hydrogen bonds might also affect the three different absorption property characters FQs.

Supplementary Information The online version contains supplementary material available at https://doi.org/10.1007/s13399-020-01222-x.

Acknowledgments We are grateful to Mr. Ueyama of Kyowakiden Co., Ltd. for taking the SEM image of the biochar. We especially thank the technical staff of the Renewable Energy Research Center of Maejo University. They kindly helped use the kiln to pyrolyze the corncob biochar.

Funding This work was partially supported by JSPS KAKENHI Grant Number 20K20640.

Compliance with ethical standards

Competing interests The authors declare that they have no competing interests.

References

1. Lien LTQ, Hoa NQ, Chuc NTK, Thoa N, Phuc H, Diwan V, Dat N, Tamhankar A, Lundborg C (2016) Antibiotics in wastewater of a rural and an urban hospital before and after wastewater treatment, and the relationship with antibiotic use-a one year study from Vietnam. Int J Environ Res Public Health 13:1–13. https://doi.org/10.3390/ijerph13060588
2. Martins AF, Vasconcelos TG, Henriques DM, Frank CS, König A, Kümmerer K (2008) Concentration of ciprofloxacin in Brazilian hospital effluent and preliminary risk assessment: a case study. Clean Soil, Air, Water 36:264–269. https://doi.org/10.1002/clen.200700171
3. Diwan V, Tamhankar AJ, Khandal RK, Sen S et al (2010) Antibiotics and antibiotic-resistant bacteria in waters associated with a hospital in Ujjain, India. BMC Public Health 10:414
4. Riaz L, Mahmood T, Khalid A, Rashid A, Ahmed Siddique MB, Kamal A, Coyne MS (2018) Fluoroquinolones (FQs) in the environment: a review on their abundance, sorption and toxicity in soil. Chemosphere 191:704–720. https://doi.org/10.1016/j.chemosphere.2017.10.092
5. Attallah OA, Al-Ghobashy MA, Nebsen M, Salem MY (2017) Adsorptive removal of fluoroquinolones from water by pectin-functionalized magnetic nanoparticles: process optimization using a spectrofluorimetric assay. ACS Sustain Chem Eng 5:133–145. https://doi.org/10.1021/acssuschemeng.6b01003
6. Conkle JL, Lattao C, White JR, Cook RL (2010) Competitive sorption and desorption behavior for three fluoroquinolone antibiotics in a wastewater treatment wetland soil. Chemosphere 80:1353–1359. https://doi.org/10.1016/j.chemosphere.2010.06.012
7. Meng F, Gao G, Yang TT, Chen X, Chao Y, Na G, Ge L, Huang LN (2015) Effects of fluoroquinolone antibiotics on reactor performance and microbial community structure of a membrane bioreactor. Chem Eng J 280:448–458. https://doi.org/10.1016/j.cej.2015.06.025
8. Nguyen TT, Bui XT, Dang BT, Ngo HH, Jahng D, Fujioka T, Chen SS, Dinh QT, Nguyen CN, Nguyen PTV (2019) Effect of ciprofloxacin dosages on the performance of sponge membrane bioreactor treating hospital wastewater. Bioresour Technol 273:573–580. https://doi.org/10.1016/j.biortech.2018.11.058
9. Kraemer SA, Ramachandran A, Perron GG (2019) Antibiotic pollution in the environment: from microbial ecology to public policy. Microorganisms 7:1–24. https://doi.org/10.3390/microorganisms7060180
10. Zhao J, Liang G, Zhang X, Cai X, Li R, Xie X, Wang Z (2019) Coating magnetic biochar with humic acid for high efficient removal of fluoroquinolone antibiotics in water. Sci Total Environ 688:1205–1215. https://doi.org/10.1016/j.scitotenv.2019.06.287
11. Cheng D, Ngo HH, Guo W, Chang SW, Nguyen DD, Li J, Ly QV, Nguyen TAH, Tran VS (2020) Applying a new pomelo peel derived biochar in microbial fell cell for enhancing sulfonamide antibiotics removal in swine wastewater. Bioresour Technol:123886. https://doi.org/10.1016/j.biortech.2020.123886
12. Wang H, Chu Y, Fang C, Huang F, Song Y, Xue X (2017) Sorption of tetracycline on biochar derived from rice straw under different temperatures. PLoS One 12:e0182776. https://doi.org/10.1371/journal.pone.0182776
13. Eduah JO, Nartey EK, Abekoe MK, Breuning-Madsen H, Andersen MN (2019) Phosphorus retention and availability in three contrasting soils amended with rice husk and corn cob biochar at varying pyrolysis temperatures. Geoderma 341:10–17. https://doi.org/10.1016/j.geoderma.2019.01.016
14. Yadav OP, Hossain F, Karjagi CG, Kumar B, Zaidi PH, Jat SL, Chawla JS, Kaul J, Hooda KS, Kumar P, Yadava P, Dhillon BS (2015) Genetic improvement of maize in India: retrospect and prospects. Agric Res 4:325–338. https://doi.org/10.1007/s40003-015-0180-8
15. Liu X, Zhang Y, Li Z, Feng R, Zhang Y (2014) Bioresource technology characterization of corncob-derived biochar and pyrolysis kinetics in comparison with corn stalk and sawdust. Bioresour Technol 170:76–82. https://doi.org/10.1016/j.biortech.2014.07.077
16. Hao F, Zhao X, Ouyang W, Lin C, Chen S, Shan Y, Lai X (2013) Molecular structure of corncob-derived biochars and the mechanism of atrazine sorption. Agron J 105:773–782. https://doi.org/10.2134/agronj2012.0311
17. Binh QA, Nguyen HH (2020) Investigation the isotherm and kinetics of adsorption mechanism of herbicide 2,4-dichlorophenoxyacetic acid (2,4-D) on corn cob biochar. Bioresour Technol Reports 11:100520. https://doi.org/10.1016/j.biteb.2020.100520
18. Peñafiel ME, Vanegas E, Bermejo D, Matesanz JM, Ormad MP (2019) Organic residues as adsorbent for the removal of ciprofloxacin from aqueous solution. Hyperfine Interact 240. https://doi.org/10.1007/s10751-019-1612-9
19. Shen Z, Zhang J, Hou D, Tsang DCW, Ok YS, Alessi DS (2019) Synthesis of MgO-coated corncob biochar and its application in lead stabilization in a soil washing residue. Environ Int 122:357–362. https://doi.org/10.1016/j.envint.2018.11.045
20. Zhang X, Zhang Y, Ngo HH, Guo W, Wen H, Zhang D, Li C, Qi L (2020) Characterization and sulfonamide antibiotics adsorption capacity of spent coffee grounds based biochar and hydrochar. Sci Total Environ:716. https://doi.org/10.1016/j.scitotenv.2020.137015
21. Kiecak A, Sassine L, Boy-Roura M, Elsner M, Mas-Pla J, le Gal la Salle C, Stumpp C (2019) Sorption properties and behaviour at laboratory scale of selected pharmaceuticals using batch

experiments. J Contam Hydrol 225:103500. https://doi.org/10.1016/j.jconhyd.2019.103500
22. Peng B, Chen L, Que C, Yang K, Deng F, Deng X, Shi G, Xu G, Wu M (2016) Adsorption of antibiotics on graphene and biochar in aqueous solutions induced by π-π interactions. Sci Rep 6:1–10. https://doi.org/10.1038/srep31920
23. Tulkens PM, Van Bambeke F, Zinner SH (2019) Profile of a novel anionic fluoroquinolone - delafloxacin. Clin Infect Dis 68:S213–S222. https://doi.org/10.1093/cid/ciy1079
24. Candel FJ, Peñuelas M (2017) Delafloxacin: design, development and potential place in therapy. Drug Des Devel Ther 11:881–891. https://doi.org/10.2147/DDDT.S106071
25. ASTM D4607–94(1999) (1999) Standard test method for determination of iodine number of activated carbon. Astm Int 94:1–5
26. Ho YS, McKay G (1998) A comparison of chemisorption kinetic models applied to pollutant removal on various sorbents. Process Saf Environ Prot 76:332–340. https://doi.org/10.1205/095758298529696
27. Akaike H (1974) A new look at the statistical model identification. IEEE Trans Automat Contr 19:716–723. https://doi.org/10.1109/TAC.1974.1100705
28. Gupta GK, Ram M, Bala R, Kapur M, Mondal MK (2018) Pyrolysis of chemically treated corncob for biochar production and its application in Cr(VI) removal. Environ Prog Sustain Energy 37:1606–1617. https://doi.org/10.1002/ep.12838
29. Dalahmeh S, Ahrens L, Gros M, Wiberg K, Pell M (2018) Potential of biochar filters for onsite sewage treatment: adsorption and biological degradation of pharmaceuticals in laboratory filters with active, inactive and no biofilm. Sci Total Environ 612:192–201. https://doi.org/10.1016/j.scitotenv.2017.08.178
30. Mianowski A, Owczarek M, Marecka A (2007) Surface area of activated carbon determined by the iodine adsorption number. Energy Sources, Part A Recover Util Environ Eff 29:839–850. https://doi.org/10.1080/00908310500430901
31. Rodriguez A, Lemos D, Trujillo YT, Amaya JG, Ramos LD (2019) Effectiveness of biochar obtained from corncob for immobilization of lead in contaminated soil. J Heal Pollut 9:13–21. https://doi.org/10.5696/2156-9614-9.23.190907
32. Spiess A-N, Neumeyer N (2010) An evaluation of R2 as an inadequate measure for nonlinear models in pharmacological and biochemical research: a Monte Carlo approach. 1–11
33. Mutavdžić Pavlović D, Ćurković L, Grčić I, Šimić I, Župan J (2017) Isotherm, kinetic, and thermodynamic study of ciprofloxacin sorption on sediments. Environ Sci Pollut Res 24:10091–10106. https://doi.org/10.1007/s11356-017-8461-3
34. Do DD (1998) Adsorption analysis: equilibria and kinetics
35. Zhuang Y, Yu F, Ma J, Chen J (2015) Adsorption of ciprofloxacin onto graphene-soy protein biocomposites. New J Chem 39:3333–3336. https://doi.org/10.1039/c5nj00019j
36. Khokhar TS, Memon FN, Memon AA, Durmaz F, Memon S, Panhwar QK, Muneer S (2019) Removal of ciprofloxacin from aqueous solution using wheat bran as adsorbent. Sep Sci Technol 54:1278–1288. https://doi.org/10.1080/01496395.2018.1536150
37. Cavallo G, Metrangolo P, Milani R, Pilati T, Priimagi A, Resnati G, Terraneo G (2016) The halogen bond. Chem Rev 116:2478–2601. https://doi.org/10.1021/acs.chemrev.5b00484
38. Xiao F, Pignatello JJ (2015) π+-π Interactions between (hetero)aromatic amine cations and the graphitic surfaces of pyrogenic carbonaceous materials. Environ Sci Technol 49:906–914. https://doi.org/10.1021/es5043029
39. Chen Z, Xiao X, Chen B, Zhu L (2015) Quantification of chemical states, dissociation constants and contents of oxygen-containing groups on the surface of biochars produced at different temperatures. Environ Sci Technol 49:309–317. https://doi.org/10.1021/es5043468
40. Lawrinenko M, Laird DA (2015) Anion exchange capacity of biochar. Green Chem 17:4628–4636. https://doi.org/10.1039/c5gc00828j
41. Bassetti M, Righi E, Pecori D, Tillotson G (2018) Delafloxacin: an improved fluoroquinolone developed through advanced molecular engineering. Future Microbiol 13:1081–1094. https://doi.org/10.2217/fmb-2018-0067
42. Carabineiro SAC, Thavorn-Amornsri T, Pereira MFR et al (2012) Comparison between activated carbon, carbon xerogel and carbon nanotubes for the adsorption of the antibiotic ciprofloxacin. Catal Today 186:29–34. https://doi.org/10.1016/j.cattod.2011.08.020
43. Goyne KW, Chorover J, Kubicki JD, Zimmerman AR, Brantley SL (2005) Sorption of the antibiotic ofloxacin to mesoporous and nonporous alumina and silica. J Colloid Interface Sci 283:160–170. https://doi.org/10.1016/j.jcis.2004.08.150
44. Zhao X, Ouyang W, Hao F, Lin C, Wang F, Han S, Geng X (2013) Properties comparison of biochars from corn straw with different pretreatment and sorption behaviour of atrazine. Bioresour Technol 147:338–344. https://doi.org/10.1016/j.biortech.2013.08.042
45. Laine J, Simoni S, Calles R (1991) Preparation of activated carbon from coconut shell in a small scale cocurrent flow rotary kiln. Chem Eng Commun 99:15–23. https://doi.org/10.1080/00986449108911575
46. L.D.Landau, E.M.Lifshitz (1987) Fluid mechanics: volume 6 (course of theoretical physics). Pergamon Press